Energy partitioning in the reaction $^{16}O(^1D)+H_2\ ^{18}O \rightarrow {}^{16}OH+{}^{18}OH$. II. The distribution of ^{16}OH and ^{18}OH

K. -H. Gericke and F. J. Comes

Institut für Physikalische and Theoretische Chemie, Universität Frankfurt am Main, Robert-Mayer-Strasse 11, 6000 Frankfurt am Main 1, West Germany

R. D. Levine

Department of Physical Chemistry, The Hebrew University, Jerusalem, Israel
(Received 2 December 1980; accepted 11 February 1981)

The reaction of $O(^1D)$ with water proceeding to two OH molecules has been studied by isotopic labeling of the oxygen atom in the water molecule in order to distinguish between the two chemically identical product molecules and to determine the product state distribution. A large fraction (~ 0.6) of the available energy is released as translation. The vibrational energy is preferentially channeled into the new (^{16}OH) bond, and the ^{16}OH vibrational distribution is "hotter" than that expected on prior (microcanonical) grounds. The opposite is true for the ^{18}OH (old bond), which is produced almost exclusively (> 0.9) in the ground vibrational state. The rotational energy is, however, equipartitioned among the two bonds. For each vibrational manifold, the rotational distribution is well characterized by a linear surprisal. Using a reduced variable, the rotational surprisal parameter is found to be independent of the vibrational state. Due to the high fraction of available energy released as translation, the fraction of energy in the rotation (~ 0.2) is less than expected on prior grounds and the surprisal parameter is positive. The ratio of the rotational surprisal parameters determined for ^{16}OH and ^{18}OH by surprisal analysis is in close agreement with that predicted by the equipartitioning of the rotational energy between the two OH molecules. The OH was found to be statistically distributed between its two possible spin states.

INTRODUCTION

Besides their importance in combustion, OH radicals play a significant role in atmospheric chemistry.[1] A major production mechanism in the earth's atmosphere is the reaction of metastable oxygen atoms $O(^1D)$ with water molecules

$$O(^1D) + H_2O \rightarrow OH + OH\ . \qquad (1)$$

The $O(^1D)$ atoms are formed by photodissociation of atmospheric ozone. Hydroxyl molecules are, therefore, a direct product of the photochemical activity of the sun. The OH radical also exists in interstellar clouds, and it is well known that these molecules are the origin of strong 18 cm maser radiation.[2]

Reaction (1) is known to be very fast[3] and the activation energy is expected to be quite small. The reaction is strongly exothermic ($\Delta H \simeq -29$ kcal/mol). In this paper we report the vibrational and rotational energy disposal using rotationally resolved resonance absorption of the nascent OH molecules. Oxygen atoms in their first excited electronic state were produced by photolysis of ozone.[4] The water molecules had a thermal distribution of internal and translational energies.

Energy disposal has been extensively studied for three center, atom–diatom reactions. Reaction (1) provides, however, an example where the internal states of both product molecules can be probed. Furthermore, the simple structure of the OH molecule allows a complete analysis of the products' state distribution including such fine details as the distribution of the different Λ components and of the electron and nuclear spins. It is of further interest that the two product molecules are chemically identical. In the picture of a direct interaction model one of the two OH radicals represents the old bond from the water molecule, whereas the other one is from the newly formed bond. We therefore need a procedure to identify the two OH radicals, which is possible by isotopic labeling of one of the oxygen atoms. The product molecules will then be ^{18}OH (old bond) and ^{16}OH (new bond). It is not expected that the small difference in mass, which only slightly influences the velocity and the zero point energy, will have any detectable effect on the observed energy distributions. The results reported here and in a sequel study[5] therefore offer an opportunity for a detailed comparison with theory for the more challenging case of four-body dynamics. That the task is not hopeless is shown, for example, by the observation that, as expected, the vibrational energy is preferentially channelled into the new bond. Additional systematics are revealed by surprisal analysis, as is discussed below.

The following discussion will concentrate mainly on the gross structure of the energy partitioning to show the participation of the two different OH bonds in the product state distribution. The finer details of the energy disposal in the reaction will be discussed in a forthcoming paper.[5]

EXPERIMENTAL

The study of the energy partitioning in an elementary chemical reaction requires that the product molecules be observed in their nascent distribution, i.e., they

 0021-9606/81/116106-07$01.00

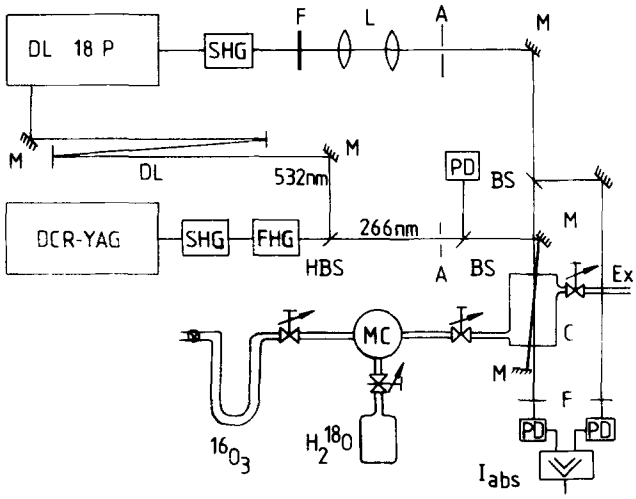

FIG. 1. Schematic diagram of the experimental set up. A: aperture; BS: beam splitter; C: chamber; DCR-YAG: Q-switched Nd: YAG laser; DL18P: pressure tuned dye laser; DL: delay line; Ex: exhaust; F: filter; HBS: harmonic beam splitter; L: lens; M: mirror; MC: mixing chamber; PD: photo diode; S (F) H G: second (fourth) harmonic generator.

have to be observed under collision free conditions. An adequate experimental procedure is the use of molecular beams. In the case of strongly reactive $O(^1D)$ atoms this procedure is not practicable; therefore a fast photochemical production–detection cycle, which is provided by nanosecond spectroscopy, has been used to study the unperturbed product state distribution.[6] For this purpose, $O(^1D)$ atoms are formed by pulse photolysis of ozone with the fourth harmonic of a Nd-YAG laser (pulse width 6 ns) at 266 nm. The second harmonic of the laser is used to pump a tunable dye laser. Its frequency is further doubled to obtain tunable radiation in the UV (pulse width 5 ns) to monitor the OH radicals. In order to correlate the $O(^1D)$ production time exactly with the OH detection time both pulses, the fourth harmonic photolysis pulse as well as the second harmonic pump pulse, are extracted from the same laser system simultaneously.

The complete set of reactions describing the OH production is given in Reactions (2) and (3):

$$^{16}O_3 + h\nu\ (266\ \text{nm}) \rightarrow {}^{16}O(^1D) + {}^{16}O_2(^1\Delta_g)\ , \qquad (2)$$

$$^{16}O(^1D) + H_2{}^{18}O \rightarrow {}^{16}OH + {}^{18}OH\ . \qquad (3)$$

As the excited oxygen atoms in the system need a certain time to react with water the second harmonic of the YAG laser is optically delayed at a delay time of 10 ns. It is an important consequence of this technique that the two laser pulses are exactly correlated to each other in time and this jitter free operation has a strong positive effect on the signal to noise ratio. This stems from the fact that in order to observe nascent OH radicals we have to operate at delay times necessarily shorter than the collision time. But in this time regime of the progressing reaction, there is a strong time dependence in the radical concentration which makes their detection sensitive to any jitter in the production–detection cycle. Ozone and water were slowly pumped through the reaction cell at constant pressures of 2 and 10 Torr at room temperature. According to the rate constant of Reaction (1), the $1/e$ time of the reaction is 13 ns under these conditions.[3] Both pressures were controlled by means of a capacitance manometer and the ozone concentration was additionally measured by its absorption of UV radiation at the specific UV laser wavelength. Water samples were 99% $H_2{}^{18}O$; ozone was produced in the usual way.[7]

The experimental setup shown in Fig. 1 consists of the laser system, the sample flowing system, and the detection system. The detection of the nascent OH radicals is performed by use of the absorption of their resonance transition ($A\,^2\Sigma - X\,^2\Pi$) in the region above 300 nm. The dyes to produce the respective first harmonic radiation were Rd B, Rd 101 (Lambda Physics) and cresyl violet.

The use of time-resolved absorption instead of the commonly applied fluorescence technique directly provides the population numbers of the OH in the specific rotational and vibrational states. To compensate for intensity fluctuations, the monitoring laser beam is split into two beams with one of them bypassing the cell (Fig. 1). Both signals are monitored by UV diodes but only the differential signal is registered and amplified. A brief description of the circuit is given in the legend of Fig. 2. The signal is stored and averaged by a boxcar integrator and registered by a recorder.

A further advantage of the use of the absorption technique is the possibility to monitor OH in higher vibrational states than $v'' = 1$. Due to the respective Franck–Condon factors the (2–2) $X \rightarrow A$ transition has to be used for detection. But the lifetime of $A\,^2\Sigma^+$ ($v'' = 2$) is reduced by a factor of 5–10 due to predissociation of OH in this state.[8] This reduces the fluorescence efficiency effectively, but does not have any detectable effect on the absorption linewidth so that the absorption technique is still very well applicable.

There is also great advantage in the application of the method to the study of relaxation phenomena because the quenching of the upper excited states does not influence the results.

The pressure tuned dye laser has a bandwidth which

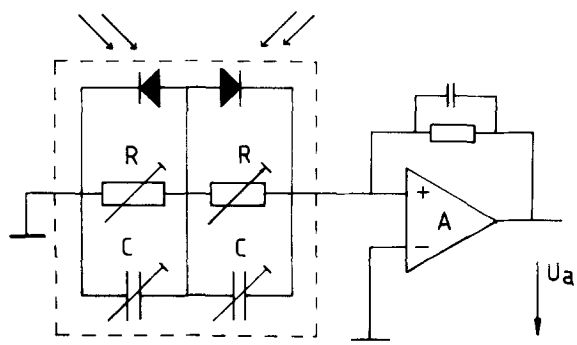

FIG. 2. Schematic diagram of differential photodiode detector. The two photodiodes in the circuit are operating as photoelements. R and C are variable, which is necessary for linear operation.

was measured to be $\Delta\nu = 1.5$ GHz with the aid of an external etalon. The doppler width of the OH transitions at room temperature is 3 GHz, which was controlled by laser absorption. The absorption line profiles of the OH produced in the reaction were measured, thus permitting the temperature of the velocity distribution of the products to be determined.

The positions of the absorption lines, as well as the oscillator strengths of the respective transitions, were taken from the literature.[9-13] Corrections for transition probabilities of ^{18}OH were made only by considering the mass effect. In the following the spectroscopic terminology of Dieke *et al.* will always be used.[9] An additional result of the treatment of the spectroscopic data is a set of molecular constants for the upper and lower electronic states of the ^{18}OH molecule.[14]

Some considerations should be given concerning a few important parameters which might influence the quality of the experimental results. The diameter of the monitoring UV beam is always kept much smaller than the diameter of the photolysis beam (1 mm/7 mm), so that the former beam is totally embedded in the latter one. The linearity of photodissociation as function of laser intensity was controlled by the linear absorption of the OH. The degree of photodissociation was chosen such that the OH absorption never exceeded 25%. The laser intensity of the OH monitoring beam was always kept at a value one order of magnitude below any detectable saturation effect.

A small section of the observed OH absorption spectrum is shown in Fig. 3. The spectrum contains absorption lines of the $v'' = 0$ vibrational state for both isotopic molecules. The isotopic lines are well separated from each other. Figure 4 is a representation of an OH absorption line taken at lower scanning speed, from which the line width can be determined. It is seen from the figure that the absorption line width greatly exceeds the laser linewidth.

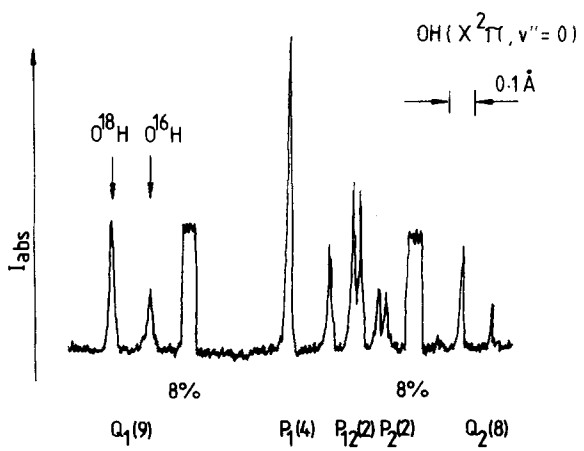

FIG. 3. Section of OH absorption spectrum $A\,^2\Sigma \leftarrow X\,^2\Pi$ for the (0–0) band. Resolution is better than 0.05 cm^{-1}. The 8% peak is a calibration mark.

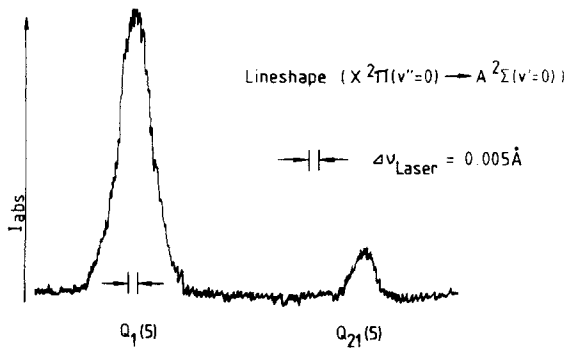

FIG. 4. Line shape of the absorption line Q_1 (5) for the (0–0) band. Resolution better than 0.05 cm^{-1}.

RESULTS

In an earlier paper (hereafter called I)[15] the energy partitioning in Reaction (1) has been discussed without considering in detail the old and the new bond. With the use of the isotopic labeling technique it is now possible to determine exactly the origin of a given hydroxyl molecule. The results are summarized in Table I, showing the partitioning of energy among the different vibrational states of OH. Only 20% of the total available energy is deposited in the vibrational degree of freedom. The same amount is in the rotational degree of freedom and 60% of the energy is released in translation. In I we described the rotational distribution in $v'' = 0$ and $v'' = 1$ by a temperature distribution with a deviation from this behavior for only the lowest four to five rotational states. We know from further experiments[5] that under a fourfold reduced collision probability, as compared to the present case, the additional contribution is mostly from rotational relaxation. That rotational relaxation proceeds so effectively is a very important finding. There is strong evidence that collisions with quantum jumps $\Delta J > 1$ are possible, transfering considerable energy.

In the light of the new experiments we have made a detailed analysis of the rotational distributions in order to investigate the participation of the new and the old bond in this important reaction. As the technology which was applied also permits monitoring the OH molecules in the vibrational state $v'' = 2$ we could observe practically all of the OH molecules formed in Reaction (3).

Vibrational energy

Figure 5 shows the relative fraction of $^{18}OH(^2\Pi, J'', v'')$ molecules at different rotational levels of the same

TABLE I. Distribution of the total OH molecules among the different vibrational states.

v''	$N(v)$
0	69
1	22
2	9

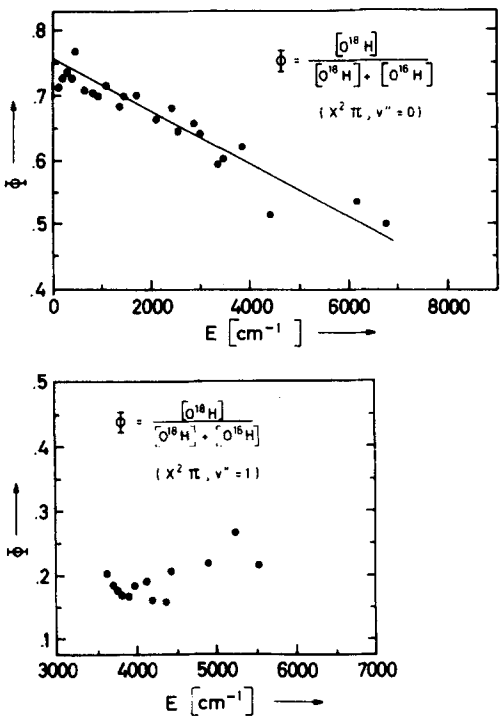

FIG. 5. Percentage of ^{18}OH in each rotational level vs the rotational energy. (Experimental conditions: $P_{H_2O} = 10$ Torr, $P_{O_3} = 2$ Torr, delay time 10 ns. The same conditions obtain for Figs. 6–8). (a) $v = 0$; (b) $v = 1$.

vibrational manifold. Figure 5(a) represents the results for the $v'' = 0$ manifold. The results shown are the sum of the contributions for the $X\,^2\Pi_{3/2}$ and $X\,^2\Pi_{1/2}$ states. There is no significant effect from electron spin. It is seen that the fractional contribution of $^{18}OH(^2\Pi, J'', v'' = 0)$ is higher at the low rotational states and decreases for higher ones. Using these results and the data from paper I we can now calculate that 46% of the total OH molecules produced in Reaction (3) are ^{18}OH molecules in the $v'' = 0$ state or 92% of all ^{18}OH formed are in the vibrational ground state. Then, the contribution of ^{18}OH to the population in $v'' = 1$ and 2 must be very low. The results for the vibrational state $v'' = 1$ are given in Fig. 5(b), showing the contribution of ^{18}OH to the overall production of OH in each rotational state. We see that the participation of ^{18}OH radicals is drastically reduced in favor of ^{16}OH. The exothermicity of the reaction is sufficient to populate the vibrational state $v'' = 2$ of OH but not $v'' = 3$. To within the detection limit (which in this case was 10% of the ^{16}OH concentration), only ^{16}OH is formed in the $v'' = 2$ state. The results show that 92% of the total ^{18}OH is in $v'' = 0$. Only 8% are found in $v'' = 1$ and less than 1% are in $v'' = 2$. The conclusion that the old bond is vibrationally cold is therefore a good approximation. The corresponding distribution for ^{16}OH vibrational states is 46%, 36%, and 18% in $v'' = 0$, 1, and 2, respectively. The vibrational energy channelled into the new bond is significantly higher.

Assuming that quantum states of all isoenergetic products are formed with the same rate one can readily compute the fractional number density of OH molecules in any given vibrational state. The results are 71%, 24%, and 5% for $v'' = 0$, 1, and 2, respectively. The vibrational energy distribution in the new bond is thus "hotter" (i.e., has a higher mean energy) than that expected on prior grounds and conversely for the old bond.

Rotational distributions

The rotational state distribution in the different vibrational manifolds is quite broad and (apart from the very low J's where collisional relaxation effects are most important[16]), closely resembles a thermal distribution. When the population in a given $v''J''$ level is summed over all the vibrational states it is found that the total population of a given rotational quantum number is very nearly equal for the two isotopic species (Table II). The only significant deviation is at high J's. But this comparison is less reliable because the absorption intensities for the respective transitions are a few orders of magnitude smaller than at the low J values.

SURPRISAL ANALYSIS

The experimental results provide a fully resolved rotational distribution of the OH molecules. As a first step towards an understanding of the collision dynamics we report the results of a surprisal analysis[17] of these distributions.

The spectroscopic detection technique, when used under collision free conditions, monitors the number density of the product molecules.[18] To perform a surprisal

TABLE II. Population of ^{16}OH and ^{18}OH in the different rotational states computed using the surprisal parameters of Table III.

J	$N(J)$ ^{16}OH	$N(J)$ ^{18}OH[a]
0.5	1.59	1.72
1.5	6.73	7.37
2.5	8.94	9.77
3.5	10.14	11.02
4.5	10.43	11.24
5.5	10.04	10.60
6.5	9.24	9.67
7.5	8.21	8.39
8.5	7.12	7.07
9.5	6.03	5.80
10.5	5.14	4.78
11.5	4.02	3.56
12.5	3.22	2.72
13.5	2.52	2.01
14.5	1.93	1.45
15.5	1.44	1.02
16.5	1.06	0.70
17.5	0.76	0.47
18.5	0.54	0.30
19.5	0.37	0.20
20.5	0.28	0.13
21.5	0.18	0.10

[a]For the very low J's the actual $N(J)$ values considered in this table are slightly higher than computed from the surprisal parameters of Table III.

analysis it is, therefore, necessary to use a number density (rather than the more usual flux density) prior distribution. When the translational energy is well defined, the required changes are trivial. Consider a single products internal state or a group of g_n degenerate internal states. The usual, flux density prior $P^0(n)$ is given by

$$P^0(n) \propto g_n E_T^{1/2} , \tag{4}$$

where E_T is the final translational energy. Dividing by the final velocity to obtain the number density, the prior distribution is

$$N^0(n) \propto g_n . \tag{5}$$

In other words, at a given total energy the prior number density is uniform for all products' *internal* quantum states, or all products' internal quantum states are formed at the same number density.

While the present experimental results have not been obtained at a sharp value of the reagents' energy, the large value of the exoergicity (−28.7 kcal/mol) implies that the spread in the energy available to the products (due to the spread in the energy of the reactants) is small.

For Reaction (3), the prior number density for producing both OH molecules in a given rovibrational state is, using Eq. (5),

$$N^0(J, v, L, u) \propto (2J+1)(2L+1) . \tag{6}$$

In Eq. (6) and throughout this section we shall use J, v and L, u to denote the rotational and vibrational levels of the one and of the other OH molecule, respectively. It follows that, within given vibrational manifolds, the prior number density rotational distribution $N^0(J, L\,|u, v)$ is

$$N^0(J, L\,|u, v) \propto (2J+1)(2L+1) . \tag{7}$$

The experimental results do not conform to the prior expectations as given by Eq. (7). To account for the deviance from the prior, we introduce the same constraint which obtains in reactive atom–diatom collisions.[19] The only modification is that here the same constraint is imposed for each OH molecule. The joint rotational distribution is then of the form

$$N(J, L\,|u, v) = (2J+1)(2L+1) \times \exp\left[-\Theta_R \frac{E_J}{E - E_v} - \Theta'_R \frac{E_L}{E - E_u}\right] \Big/ Q . \tag{8}$$

Here, Θ_R and Θ'_R are the rotational suprisal parameters for the two OH molecules and E is the total energy available to the products. Q is the normalizing factor that insures that $N(J, L\,|u, v)$ is properly normalized

$$\sum_L \sum_J N(J, L\,|u, v) = 1 . \tag{9}$$

The experimental results show that the rotational distribution is rapidly declining at high J's (or L's), i.e., that Θ_R is positive. Hence, in evaluating Q one can disregard the limitations imposed by the conservation of energy and sum over J and L up to infinity. The distribution of either ^{16}OH or ^{18}OH rotational states in a given vibrational manifold is then given by

TABLE III. Distribution of ^{18}OH and ^{16}OH among the different vibrational states and the results of surprisal analysis of the rotational distributions.

	^{18}OH			^{16}OH		
v	$N(v)$	Θ_R	T_v (K)	$N(v)$	Θ_R	T_v (K)
0	0.92	7.5	1.900	0.46	5.5	2.600
1	0.08	7.7	1.200	0.36	5.8	1.600
2	<0.01			0.18	5.9	600

$$N(J\,|v) = (2J+1) \exp\left[-\Theta_R \frac{E_J}{E - E_v}\right] \Big/ Q_R(v) , \tag{10}$$

where

$$Q_R(v) = \sum_J (2J+1) \times \exp\left[-\Theta_R \frac{E_J}{E - E_v}\right] \simeq (E - E_v)/B_e\Theta_R . \tag{11}$$

Here, B_e is the rotational constant of OH and the sum in Eq. (11) has been evaluated by approximating it by an integral.

The distribution Eq. (10) is indeed "thermal-like" and by writing the exponential factor as $\exp(-E_J/kT_v)$, the parameter T_v is given by

$$kT_v = (E - E_v)/\Theta_R , \tag{12}$$

where k is Boltzmann's constant. It should be clearly stated, however, that at thermal equilibrium the rotational temperature is the same for all vibrational manifolds. The experimental results (cf. Table III) are, rather, that it is Θ_R which is constant, while T_v differs [in a systematic fashion, as given by Eq. (12)] for the different vibrational manifolds.

Figures 6–8 show a plot of the surprisal $-\ln[N(J\,|v)/N^0(J\,|v)]$ versus E_J, for $v=0$, 1, and 2 for both ^{16}OH and ^{18}OH. Except for the low J's, where there are deviations due to collision-induced relaxation, the linear functional dependence implied by Eq. (10) is well satisfied. The results are summarized in Table III. As is quite evident, Θ_R is independent of the vibrational state. The results also explain the failure to detect the ^{18}OH molecules in the $v=2$ state. According to Eq. (12), the value of T_v in that manifold would be about 450 K. In other words, very few rotational states would be populated.

As an additional check of the functional form Eq. (10), we have used it to compute the relative population $N(J)$ in the different rotational states

$$N(J) = \sum_v N(J\,|v) N(v) , \tag{13}$$

using the values of $N(v)$ from Table III. The results for both ^{16}OH and ^{18}OH are shown in Table II. In agreement with experiment, it is seen that except at the high J values, $N(J)$ is very nearly the same for both ^{16}OH and ^{18}OH.

The values of Θ_R found for ^{16}OH and ^{18}OH, (cf. Table III), are significantly different, as is the vibrational en-

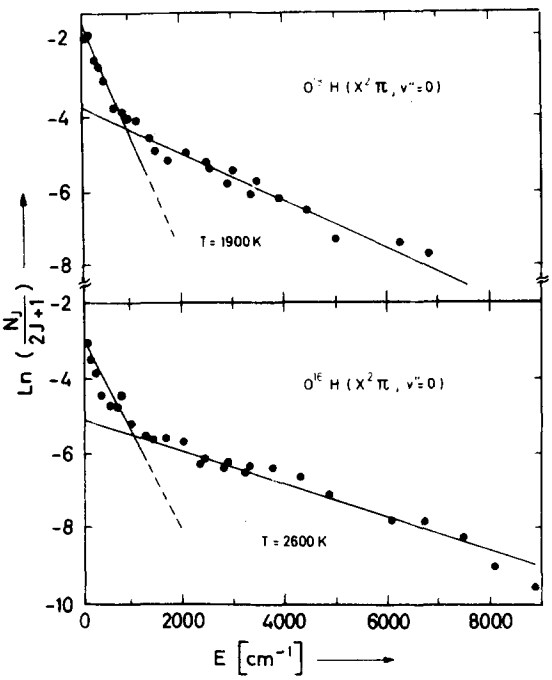

FIG. 6. Distribution of produced ^{18}OH (a) and ^{16}OH (b) in the rotational states of $^2\Pi_{3/2,1/2}$ ($v''=0$) for both Λ levels. The plot is of $\ln[N(J)/(2J+1)]$ vs the rotational energy so that the slope is $-1/kT_v$. The value of T_v is shown.

ergy disposal. We can reconcile these two separate observations as follows. The mean rotational excitation $\langle E_J\rangle$,

$$\langle E_J\rangle = \sum_v \sum_J E_J\, N(v,J)\ ,$$
$$= \sum_J E_J\, N(J) \qquad (14)$$

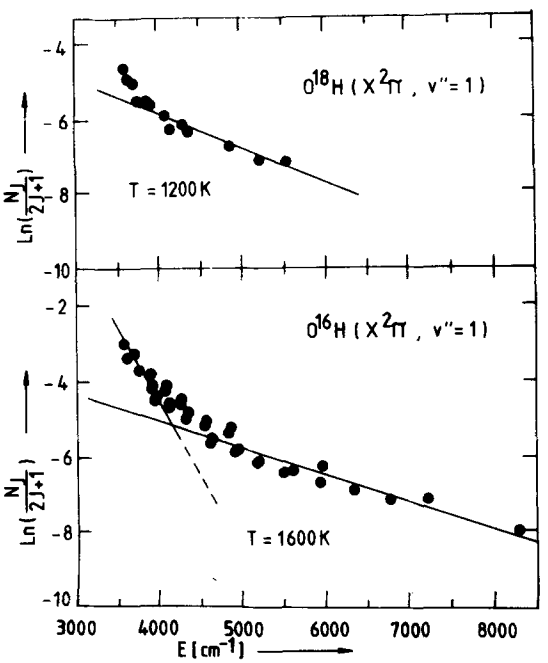

FIG. 7. Distribution of produced ^{18}OH (a) and ^{16}OH (b) in the rotational states of $^2\Pi_{3/2,1/2}$ ($v''=1$) for both Λ levels. The plot is of $\ln[N(J)/(2J+1)]$ vs the rotational energy so that the slope is $-1/kT_v$. The value of T_v is shown.

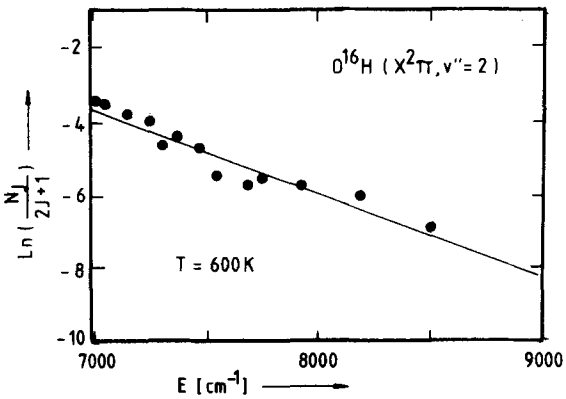

FIG. 8. Distribution of produced ^{16}OH in rotational states of $^2\Pi_{3/2,1/2}$ ($v''=2$) for both Λ levels (Boltzmann representation).

is found to be the same, ($\sim 0.2E$), for both ^{16}OH and ^{18}OH. For the functional form Eq. (10) we have that

$$\sum_J \left(\frac{E_J}{E-E_v}\right) N(J\,|\,v) \simeq 1/\Theta_R\ , \qquad (15)$$

where the approximation is that of replacing summation of J by integration over E_J. Using Eq. (15), one can evaluate $\langle E_J\rangle$ as follows:

$$\langle E_J\rangle = \sum_v \sum_J E_J\, N(J,v)$$
$$= \sum_v (E-E_v) \sum_J \left(\frac{E_J}{E-E_v}\right) N(J\,|\,v) N(v)$$
$$= \Theta_R^{-1} \sum_v (E-E_v) N(v)$$
$$= (E - \langle E_v\rangle)/\Theta_R\ . \qquad (16)$$

In other words, the equipartitioning of the rotational energy between ^{16}OH and ^{18}OH,

$$\langle E_J(^{16}OH)\rangle = \langle E_J(^{18}OH)\rangle\ , \qquad (17)$$

necessarily implies that ^{16}OH, which has a higher value of $\langle E_v\rangle$, must have a lower value of Θ_R. Explicitly, using Eqs. (17) and (16),

$$\frac{E - \langle E_v(^{16}OH)\rangle}{\Theta_R(^{16}OH)} = \frac{E - \langle E_v(^{18}OH)\rangle}{\Theta_R(^{18}OH)}\ , \qquad (18)$$

or in terms of the temperature parameters [cf. (12)],

$$\frac{T_v(^{18}OH)}{T_v(^{16}OH)} = \frac{E - \langle E_v(^{16}OH)\rangle}{E - \langle E_v(^{18}OH)\rangle}\ . \qquad (19)$$

The "temperature" ratio obtained from Figs. 6 and 7 is 0.73 and 0.75 for $v=0$ and 1, respectively. The value of the ratio on the right-hand side of Eq. (19), computed using $N(v)$ from Table III, is 0.73. The two rotational surprisal parameters given in Table III are thus not independent but are related by Eq. (18).

DISCUSSION

The energy partitioning in Reaction (3) shows some striking features. Most of the available energy is released in the transitional mode. The vibrational energy distribution is definitely deviant from the prior expecta-

tions. The distribution of the isotopic molecules among the different vibrational states strongly indicates a direct or impulsive type of reaction mechanism, in contrast to a long-lived collision complex or compound mechanism. In the latter case, the lifetime of the complex is long compared with the rotational period and the distinction between the "old" and "new" bonds should be lost.

The rotational energy in the different vibrational states shows a broad distribution which can be described within the error limits by a single constraint. The constrained rotational distribution can be expressed in a Boltzmann-like form. However, the resulting temperature is found to be different for the different vibrational manifolds. The origin of these variations is fully accounted for by the functional form [Eq. (10)], where Θ_R (cf. Table III) is found to be independent of the vibrational state. The very same constraint was previously identified in atom–diatom collisions.

A novel feature of the dynamics is the near equality of the total population in a given rotational state for the two diatomic products (cf. Table II)

$$[^{18}OH(J)] \simeq [^{16}OH(J)] \,, \tag{20}$$

where the square brackets denote, as usual, number densities. A particular implication of Eq. (20) is that the mean rotational energy $\langle E_J \rangle$ has the same value for ^{18}OH and ^{16}OH. This result relates the energy disposal for the two diatomic products. It should prove of particular interest to determine whether for reactions leading to two distinct diatomic products, (e.g., $H + NO_2$) give similar results.

ACKNOWLEDGMENTS

The authors are grateful to the DFG for financial support and to M. Nuss for his assistance in part of the measurements.

[1] J. Heicklen, *Atmospheric Chemistry* (Academic, New York, 1976); M. Nicolet, Rev. Geophys. Space 13, 593 (1975).
[2] A. H. Cook, *Celestial Masers* (Cambridge University, London, 1977).
[3] J. A. Davidson, H. I. Schiff, G. E. Streit, S. R. McAffee, A. L. Schmeltekopf, and C. J. Howard, J. Chem. Phys. 67, 5021 (1977), K. H. Gericke and F. J. Comes, Chem. Phys. Lett. (1981) (in press).
[4] R. K. Sparks, L. R. Carlson, K. Shobatake, M. L. Kowalczyk, and Y. T. Lee, J. Chem. Phys. 72, 1401 (1980); C. E. Fairchild, E. J. Stone, and G. M. Lawrence, *ibid.* 69, 3632 (1978).
[5] K.-H. Gericke and F. J. Comes (to be published).
[6] K.-H. Gericke, G. Ortgies, and F. J. Comes, Chem. Phys. Lett. 69, 156 (1980).
[7] I. Arnold and F. J. Comes, Chem. Phys. Lett. 24, 211 (1977).
[8] R. A. Sutherland and R. A. Anderson, J. Chem. Phys. 58, 1226 (1973); K. R. German, *ibid.* 63, 5252 (1975).
[9] G. H. Dieke and H. M. Crosswhite, J. Quant. Spectrosc. Radiat. Transfer 2, 97 (1962).
[10] E. A. Moore and W. G. Richards, Phys. Scripta 3, 223 (1971).
[11] R. J. M. Bennett, Mon. Not. R. Astron. Soc. 147, 35 (1970).
[12] W. L. Dimpfl and J. L. Kinsey, J. Quant. Spectrosc. Radiat. Transfer 21, 233 (1979).
[13] C. C. Wang and D. K. Killinger, Phys. Rev. A 20, 1495 (1979).
[14] M. Nuss, K.-H. Gericke, and F. J. Comes (to be published).
[15] K.-H. Gericke and F. J. Comes, Chem. Phys. Lett. 74, 63 (1980).
[16] J. C. Polanyi and K. B. Woodall, J. Chem. Phys. 57, 1574 (1972).
[17] R. D. Levine and J. L. Kinsey, in *Atom–Molecule Collision Theory*, edited by R. B. Bernstein (Plenum, New York, 1979).
[18] J. M. Farrar and Y. T. Lee, Ann. Rev. Phys. Chem. 25, 357 (1974).
[19] R. D. Levine, B. R. Johnson, and R. B. Bernstein, Chem. Phys. Lett. 19, 1 (1973).